Image to Mesh: Spinal Ligament 3D Surface Models from Bone Volume Images and Dynamic Radiographs

Md. Abedul Haque and G. Elisabeta Marai

University of Pittsburgh, Dept. of Computer Science
Pittsburgh, USA

Abstract. At present no *in vivo* non-invasive method exists for generating subject-specific ligament meshes from medical images of human spine. Dynamic ligament meshes can help us to understand the role of ligaments in spine dynamics through simulation. In this paper, we present a semi-automatic method to reconstruct 3D ligament meshes through computational means from *in vivo* images of spine. The method uses vertebral volumetric images and motion information to predict 3D ligament meshes across motion. Generated mesh models can be used as inputs to joint simulations. Comparison against *in vitro* experimental methods shows that our models are accurate. In addition, direct quantitative analysis on our generated meshes has shown interesting insights into the joint conditions of two subjects.

Keywords: Image to mesh pipeline, ligament surface mesh, spine ligaments, medical imaging, computational method, dynamic simulation

1 Introduction

Ligament soft-tissues directly constrain the movement of the human spine, by anchoring together the adjacent vertebrae in the spine. Understanding the role of these ligaments can provide important insights into joint mechanics and lead to better understanding of joint-related injuries and diseases. An *in vivo* and non-invasive modeling technique is essential to understand the role of the spine ligaments during everyday normal functionalities. An *in vivo* non-invasive technique is also necessary for large scale experimentation with spine ligaments.

However, due to limitations in existing imaging technologies, no *in vivo* non-invasive method exists for dynamic modeling of spine ligaments. Ligament mesh creation techniques based directly on Computed Tomography (CT) or Magnetic Resonance (MR) images have been proposed for modeling soft-tissues in larger joints like the shoulder or the knee [1, 2]. Such techniques do not transfer to the spine due to the spine joint complexity and small ligament structures.

We propose a computational method for modeling the 3D surface of spine ligaments using computed tomography medical volumes and bone motion information. This approach enables us to circumvent limitations in the spine imaging

process. The intuition behind our method is that, because ligaments are soft-tissues attached to bones and they constrain bone motion directly, the bone surfaces and their position and orientation over time can be used to predict geometric features of ligaments. This approach builds on recent advances in motion tracking technology, which enable us to reconstruct bone motion from *in vivo* images. The resulting subject-specific dynamic ligament mesh models can help us to observe ligament deformation during motion. These models can also be used as inputs to joint simulation methods such as Finite Element (FE) analysis.

2 Related Work

Based on the nature of the generated models, ligament modeling techniques can be classified in the following three categories: 1. Static 2. Dynamic and 3. Quasi-static techniques.

Static or quasi-static mesh models [1–3] of large soft-tissue structures such as knee ligaments and cartilage have been generated from CT and MR images. However, the limited resolution of these imaging techniques and the complexity of spine joints make it practically impossible to apply these techniques for spine ligament modeling.

Manually generated spine ligament meshes have been used extensively in Finite Element (FE) analysis. However, the manual approach is labor intensive and time consuming which makes it impractical for real clinical application. Mesh morphing based techniques [4–6] have been developed to automate the mesh generation process of bones for FE analysis. However, these techniques cannot be applied to ligament modeling directly due to the large deformation of ligaments and the constrain imposed on ligaments by bones.

Ligament models with linear or piecewise linear mesh elements have been used in dynamic simulation of joints [7]. This method can represent more complex geometries by using analytical wrapping structures such as cylinders or spheres. Even though this method enables dynamic simulations and reduces the modeling complexity significantly, these oversimplified models cannot provide anatomically accurate insights into the ligament geometry and geometric deformations of ligaments that happen due to motion.

A quasi-static method [8] has been proposed for distal-radioulnar ligaments in the human forearm. The method generates one-dimensional ligament fiber models and uses motion information which is based on multiple static-postures over a motion sequence. In this paper, we extend this approach to use continuous motion information for creating 3D surface models of spine ligaments.

3 Materials and Methods

We propose a semi-automated approach to reconstruct ligament meshes from captured medical images by applying computational methods. Because ligament tissues are directly constrained by bone geometries and positions, we use bone

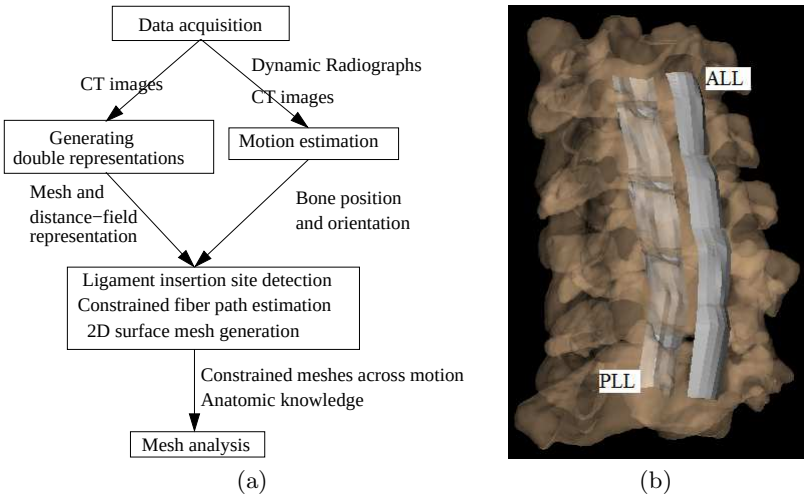

Fig. 1. (a)Method pipeline for the ligament modeling. First, bone motion information is reconstructed from 3D CT volume images and 2D dynamic radiographs. Ligament insertion sites are manually selected. Then, constrained ligament meshes are estimated across motion using the bone geometry and the motion information. Finally, ligament features are computed by analyzing the constrained geometries across motion. (b) Reconstructed Anterior Longitudinal Ligament (ALL) and Posterior Longitudinal Ligament (PLL) meshes of a subject.

geometries and positions to predict ligament models. The reconstructed models represent constrained geometries of ligaments.

Figure 1 shows our proposed method. First, accurate 3D bone geometry is captured using a static imaging technique. Next, the motion information of bones is reconstructed using an *in vivo* non-invasive model-based method. The method uses dynamic 2D X-ray images captured during motion and the bone models generated from the static volumetric images to accurately reconstruct the bone motion. Then we compute double representations (mesh and distance-field based) of the 3D bone geometry to facilitate faster computation of inter-bone joint space measurements. Ligament constrained geometries during a complete movement sequence are estimated using the hybrid representations and the motion information of bones. Then we analyze these constrained geometries to get insight into ligament geometry features. We describe each step of the pipeline in detail below.

3.1 Data Acquisition and Pre-processing

We used *in vivo* conditions and real clinical data to test our ligament modeling method. 3D bone geometries required by our modeling process were obtained from a high resolution Computed Tomography (CT) scanner (Light-Speed 16, GE Medical Systems, Waukesha, WI). CT images were segmented semi-

automatically using 3D medical imaging software to extract individual bone geometry.

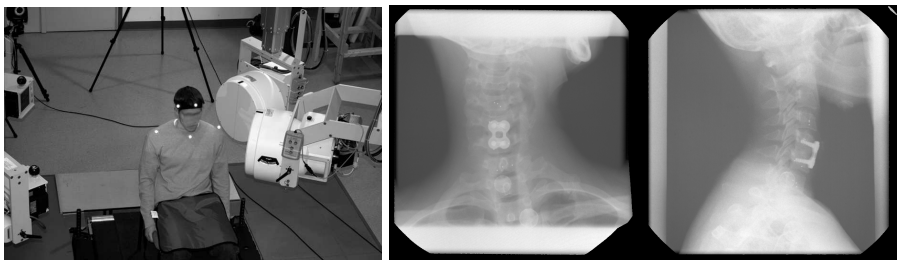

(a) (b)

Fig. 2. A dynamic stereo X-ray (DSX) system (a) was used to capture radiographs during motion. Two X-ray movies are captured from two angles using the system. (b) shows snapshots from the captured X-Ray movies [9].

3D motion information was reconstructed using our previously developed model-based hierarchical method [10, 11]. The motion reconstruction method uses a dynamic stereo X-ray (DSX) system (Figure 2) to capture high resolution X-ray images at a high frame rate. DSX utilizes two frame-synchronized imaging systems each including a 100 kW cardiac cine-radiographic generator, a 0.3/0.6 mm focal spot size X-ray tube, a 40 cm image intensifier and a high-speed camera providing 1800x2400 pixel resolution at up to 500 frames/sec with 14-bit dynamic range.

The basic premise for reconstructing bone motion is a model-based approach that matches radiographic images to a known bone shape (3D bone models obtained from the CT scans). A virtual model of the DSX imaging system is generated using the precise locations of the radiographic sources and image detectors. Simulated X-rays are passed through the bone models to produce a pair of digitally reconstructed radiographs (DRRs) on the image plane. By manipulating the bone model within a virtual radiographic system, pairs of DRRs can be generated for any bone position. By calculating image similarity measures between the actual radiographic image pairs and the DRRs, the virtual bone position and orientation can be adjusted (manually or by an optimization algorithm) to identify the position that provides the greatest match, thus determining the position of the actual bone in space. This process is repeated for each pair of the images in the motion sequence, and repeated again for each bone of interest to yield the 3D position of the joint for the entire movement.

3.2 Representations of Bone Geometry

To enable computational modeling of the ligament structures, we compute two representations (explicit mesh representation and implicit distance-field representation) of the 3D bone geometry from the CT images of bones. The bone

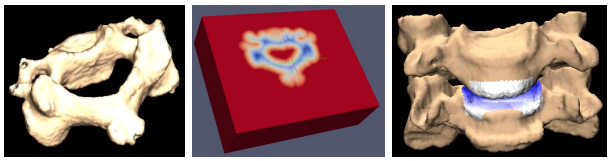

(a) (b) (c)

Fig. 3. Double representations of a bone model (a) mesh representation (b) distance field representation. Red indicates points outside the bone surface and blue indicates points inside the bone surface. The distance from the surface is mapped to the color saturation level. (c) Visualization of inter-bone joint space computed using the distance-field information.

models are segmented semi-automatically by domain experts using 3D medical imaging software (Mimics, Materialize Inc, Leuven, Belgium). A combination of segmentation techniques (e.g. region growing, threasholding) is applied and manually corrected to obtain highly accurate bone models. We did not apply any smoothing or simplification to the segmented models. The resulting mesh models have between 10k $\sim$ 20k vertices and 20k $\sim$ 50k faces per vertebra. The explicit mesh representation (Figure 3a) is used for manual identification of landmarks such as ligament insertion sites and to visually confirm the correctness of the generated models. The implicit distance-field (Figure 3b) representation [12] enables faster computation of joint-space distances (Figure 3c) such as distance between an arbitrary point in the joint space and the nearest bone surface.

We compute the mesh models using the marching cube [13] algorithm. To generate distance-field models, we applied the closest point transform method [12] on the explicit mesh representation.

3.3 Constrained Ligament Path Estimation

From the double bone representations and the reconstructed motion information, our method estimates 3D surface models of ligament path constraints. The generated 3D models represent the minimum-length ligament paths wrapped around the bone surface and constrained by the bone geometry and position.

The D surface model creation begins with ligament insertion site (the points where the ligament is attached to the bone) identification. We manually identify an array of points as ligament insertion sites for each bone. Insertion sites of a ligament contain the same number of points for all bones. A mapping function maintains the connectivity information between points of insertion sites.

To compute a ligament model, a single ligament fiber is assumed between two corresponding points of two insertion sites. The path constraint of a single fiber is basically the shortest path between its two insertion points constrained by the bone structures. As in [8], the path constraint is computed using an optimization method that exploits the distance field representations of the bones for computational efficiency.

The optimization algorithm assumes a linear segment between the two insertion points (p_0 and p_n) of a fiber. Intermediate points ($p1 \dots p_{n-1}$) are generated through sampling at uniform intervals. Then the algorithm optimizes the intermediate points to minimize the length of the path through all intermediate points under the constraint that no point is inside any bone model. To ensure efficient computation of the constraints, we use the implicit distance field representation. For any point ($p_{x,y,z}$), the distance-field representation (f) gives the distance (positive if the point is outside the bone surface and negative if the point is inside the bone surface) between the point and the nearest point on the bone surface. The optimization routine minimizes the following cost function (equation 3.1 in [8])

$$\min_{x_i,y_i,z_i} \sum_{i=0}^{n-1} \sqrt{(x_{i+1}-x_i)^2 + (y_{i+1}-y_i)^2 + (z_{i+1}-z_i)^2} \tag{1}$$

subject to $f(x_i, y_i, z_i) > 0, i = 1 \dots n-1$. Since we keep the intermediate points equally spaced along the path, $(x_{i+1} - x_i)$ is constant. Therefore, the optimization problem reduces to

$$\min_{y_i,z_i} \sum_{i=0}^{n-1} \sqrt{const + (y_{i+1}-y_i)^2 + (z_{i+1}-z_i)^2} \tag{2}$$

subject to $f(x_i, y_i, z_i) > 0, i = 1 \dots n-1$.

We use a sequential quadratic programming (SQP) method (from the high performance NAG library [14], implemented in C/C++) to solve the optimization problem. However, the optimization method is prone to converging towards local minima. To tackle this challenge, we take advantage of temporal coherence and use the computed geometry of a frame to initialize the optimization process of the neighboring frames. We found that this method converged to the correct solution successfully (on average 150 iterations required per fiber per segment of the ligament) for all frames of the motion sequences. The resulting ligament mesh consists of approximately 1400 vertices.

To generate a 3D mesh surface model, we first construct multiple interconnected fibers. Individual fiber paths are computed following the approach described above. Then we generate a uniformly distributed equal number of points along all computed fiber paths. We perform a custom triangulation on the points to generate the 3D mesh of the ligament (Figure 1b).

3.4 Model Analysis

The 3D ligament meshes generated using our method could be used as input geometries to joint simulation methods such as FEM. However, even this simple mesh representation has further uses. We show how a quantitative analysis on the 3D surface meshes can be used to get insights into the underlying ligament geometry and to extract useful measurements for comparative analysis.

Ligament	Avg. neutral length from our models	*in vitro* avg. length from literature
ALL	19.7±1.11	18.8±1.04
PLL	17.69±2.27	19.0±1.04

Table 1. Average neutral ligament length computed from the mesh models against *in vitro* results from biomed literature.

To enable quantitative analysis, we compute average length and average deflection of the 3D surfaces for all frames. Average length of a 3D surface model gives us a lower bound on the ligament length in that posture. Similarly, deflection analysis of ligaments during motion may indicate a potential unhealthy condition of the joint. We also analyze the distance between fibers of the surface meshes to see if the fiber paths bunch or bundle together along the width of the ligament models.

To compensate for subject-specific variation across subjects, we designed normalized measurements. We manually identify a set of frames from the motion sequences which resemble most a neutral posture. Measurements of all the remaining frames are normalized with respect to the measurements of these reference frames. These normalized measurements indicate changes in the ligament geometry in percentage rather than absolute values, and thus enable comparative analysis among subjects.

4 Results

Following approval from our Institutional Review Board (Pitt IRB), we applied our method on real clinical data captured from two subjects - one with healthy cervical spine and the other with a single level anterior fusion in vertebrae C5-C6. The fusion patient was tested between 6 and 7 months post surgery. We selected one healthy and one fusion patient to see how the surgery affects the ligaments and to validate that our method is applicable for inter-subject comparison. We selected the two major ligaments [15] of spine: Anterior Longitudinal Ligament (ALL) and Posterior Longitudinal Ligament (PLL) for our modeling. These continuous ligaments provide the main support in the anterior and the posterior of the spinal column.

First, we compare the average lengths of the ligament meshes in the reference frames (Table 1) of the motion sequence with the previously published neutral lengths of ligaments estimated through experimental methods on cadavers [16]. Table 1 shows that the computed mesh length is in agreement with previously published results (within the first standard deviation of our measurements for both ligaments).

Comparative Analysis. Normalized length and deflection of ligaments per segment (i.e. C3-C4, C4-C5, C5-C6 and C6-C7) were used to compare the models generated for the two subjects.

Anterior Longitudinal Ligament (ALL). Comparison on ALL can be done for one segment (C3-C4) because the fusion surgery removed ALL from

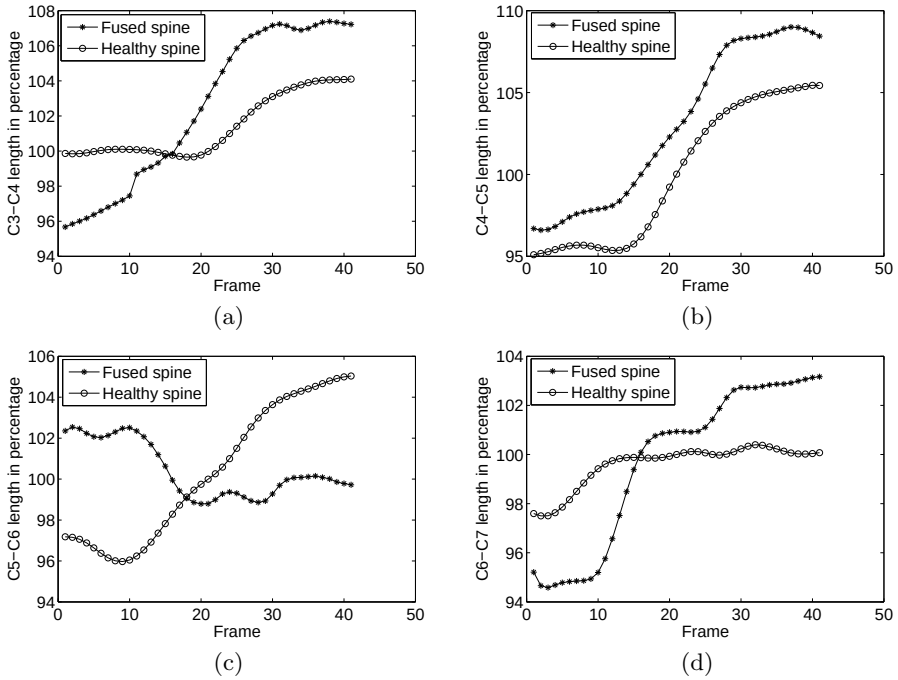

Fig. 4. Normalized length analyses across the dynamic motion range(from full extension to full flexion) for each segment of the spinal posterior ligament band for a fusion and a healthy subject. C5-C6 shows the most significant change in the length variation across the motion (c). Other segments of the spine compensate for the fusion.

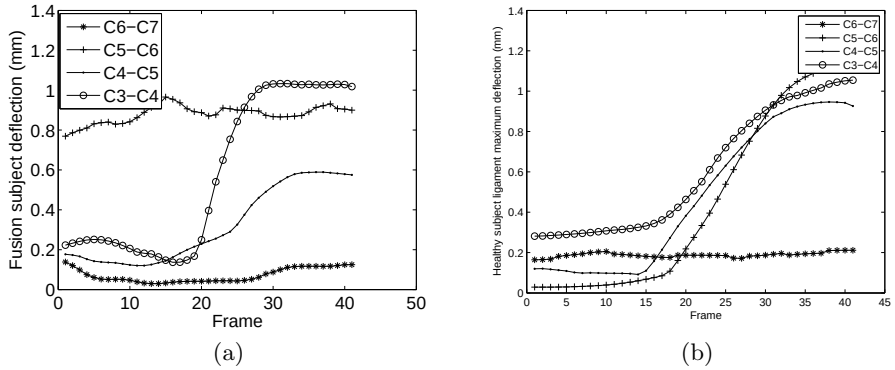

Fig. 5. Maximum deflection analyses across the dynamic motion range(from full extension to full flexion) for each segment of the spinal canal for a fusion and a healthy subject. Because of the fusion, C5-C6 ligament segment shows significant difference in the deflection. Deflection differences for the other segments are not significant.

Segment	Normalized length variation range(%)		Deflection variation range(mm)	
	Fusion	Healthy	Fusion	Healthy
C3-C4	12%	4%	0.9mm	0.8mm
C4-C5	12%	10%	0.5mm	0.9mm
C5-C6	4%	9%	0.2mm	1.1mm
C6-C7	9%	3%	0.1mm	0.05

Table 2. PLL mesh model comparison (normalized length and deflection variation) between the fusion and healthy datasets.

the fused bones. We found that the ligament features of the two subjects vary similarly. For both subjects, normalized length variation is within 18% of the reference frame length and the deflection variation is within 0.2 mm range.

Posterior Longitudinal Ligament (PLL). Normalized length analysis and deflection measurements show an interesting pattern for PLL ligament segments (Table 2). We found a significant difference between the two subjects in normalized length variation and deflection over the range of motion for the C5-C6 fusion segment (Figure 4c). For the fusion subject, other segments (i.e. C3-C4, C4-C5 and C6-C7) show increased length variation indicating more movement in these segments to compensate for the fusion in C5-C6 (Figure 4). In a healthy spine, C4-C5 and C5-C6 segments account for more motion than the C3-C4 and C6-C7 segments. Deflection variations of the segments other than C5-C6 cannot be considered significant because our bone models are created from CT images with resolution 0.3mm$\sim$0.5mm (Figure 5).

We computed the inter-fiber distances for the longitudinal ligaments across the motion sequence. Change in inter-fiber distances is an indication of interaction of ligament fibers perpendicular to the fiber direction. We did not observe any bundling of fibers and significant change in inter-fiber distances (0.05% $\sim$ 3.5% of the average width). This agrees with the anatomic knowledge that longitudinal ligament fibers are mostly oriented parallel to the length of the spine and provide almost no mechanical support perpendicular to the fiber direction.

5 Discussion and Conclusion

The results show that our image-to-mesh models are in agreement with measurements from experimental *in vitro* methods. Comparative analyses between a healthy and a fusion patient show smaller variation of ligament lengths in the fusion segment and larger variations in the surrounding segments. This indicates that our method can capture anatomically significant subject-specific features of ligaments. Because the method is mostly automatic and allows *in vivo* non-invasive modeling, it can be applied in control group studies to get insights into ligament related diseases and injuries.

Note the measurements are in general agreement with reports from *in vitro* studies, despite anatomical variation, as well as variation in procedural length

definition across studies; for example, Przybylski et al. [17] define lengths as the span over inter-vertebral discs, resulting in shorter reported lengths.

The optimization algorithm of our tool is fully automatic and requires approximately 5 minutes per frame in a standard PC (2 GHz processor, 4.00 GB RAM). The ligament geometries are pre-computed and then loaded for real-time visualization and analysis. Using parallel computation can significantly reduce the runtime of the optimization.

Our modeling pipeline requires the identification of insertion points and reference frames. This step requires less than an hour per subject (less than 50 minutes for locating insertion sites of all bones and less than 5 minutes for identifying neutral frames within the motion sequence). Please note that these manual steps are performed to the best of the user's capability. No *in vivo* approach exists today for accurate identification of these features for spine.

Our method successfully handles geometric variations of different vertebral bodies and the geometric changes due to fusion. In terms of limitations, ligament insertion sites may vary across human subjects and thus influence our mesh reconstruction. This type of insertion data, respectively ligament geometry cannot be currently acquired non-invasively for the spine. Furthermore, validation of the reconstructed meshes against *in vitro* data is challenging because ligament loading conditions and their properties change significantly when the ligaments are removed from the joint.

Our ligament models are simple 3D surfaces rather than 3D structures. We made this assumption because the thickness of longitudinal ligaments is not directly constrained with bone geometries and positions. In addition, limited resolution of the bone geometry and the accuracy level of motion information used in our method would make the small measurements of the ligament thickness (generally < 1.5 mm) insignificant.

In our approach, we have used a hierarchical model-based motion reconstruction method which has been previously reported to have sub-millimeter accuracy for *in vivo* cervical spine studies. Using alternative, lower accuracy motion reconstruction methods may affect the quality of the mesh model reconstruction.

In future, we would like to validate our method using cadaver data or by applying the method to larger joints like the knee, where MR images can capture the joint ligaments. However, validation of the reconstructed models against in-vitro data would be problematic because the ligament soft-tissue deforms significantly when dissected due to the change in loading conditions. Thus, in-vitro validation would lead to inaccurate measurements.

We would also like to analyze the uncertainty due to the identification of insertion sites and the references frames manually. Another direction of future work would be developing an automated technique to estimate the ligament insertion sites and the reference frames using anatomical features. This approach would further reduce the manual labor required for the tool.

Currently the mesh optimization run-time is a hindrance for the tool to be clinically relevant. However, the issue can be easily resolved by using more

processors or parallel implementation of the algorithm or a better optimization scheme.

In conclusion, we have designed and developed a semi-automatic method to reconstruct 3D ligament meshes from captured multimodal images of joints. The method is *in vivo* and non-invasive, and it allows subject-specific dynamic analysis of spine ligaments. The method generates anatomically accurate models and enables comparison between different subjects.

Because the method uses *in vivo* data, it can be applied in large scale experiments for validating hypotheses related to spine ligament injuries and diseases. The generated mesh models can be used as geometry inputs to FE analyses of spine. Because the manual processing is not significant, the tool has potentials for real clinical scenarios. The tool can also be very useful for biodynamics and orthopedic research.

Ethical approval. All subjects for the study signed Institutional Review Board (IRB: PRO08120294 dated 24 March 2009)-approved informed consent forms before being enrolled in the study.

Acknowledgments. We thank Scott Tashman and William Anderst (Department of Orthopaedics, University of Pittsburgh) for the spinal data acquisition and preprocessing. This work is supported by grants NSF IIS-0952720 and NIH/NIAMS R03-AR056265.

References

1. Heimann, T., Chung, F., Lamecker, H., Delingette, H.: Subject-specific ligament models: Towards real-time simulation of the knee joint. (2009) 107–119 Asclepios Project, INRIA, Sophia Antipolis, France.
2. Weiss, J., Gardiner, J., Ellis, B., Lujan, T., Phatak, N.: Three-dimensional finite element modeling of ligaments: technical aspects. Medical Engineering & Physics **27**(10) (2005) 845–61
3. Baldwin, M., Langenderfer, J., Rullkoetter, P., Laz, P.: Development of subject-specific and statistical shape models of the knee using an efficient segmentation and mesh-morphing approach. Comput Methods Programs Biomed **97**(3) (2010) 232–40
4. Bah, M., Nair, P., Browne, M.: Mesh morphing for finite element analysis of implant positioning in cementless total hip replacements. Med Eng Phys **31**(10) (2009) 1235–43
5. Sigal, I., Hardisty, M., Whyne, C.: Mesh-morphing algorithms for specimen-specific finite element modeling. J Biomech **41**(7) (2008) 1381–9
6. Sigal, I., Yang, H., Roberts, M., Downs, J.: Morphing methods to parameterize specimen-specific finite element model geometries. J Biomech **43**(2) (2010) 254–62
7. Delp, S., Anderson, F., Arnold, A., Loan, P., Habib, A., John, C., Guendelman, E., Thelen, D.: Opensim: open-source software to create and analyze dynamic simulations of movement. IEEE Trans Biomed Eng **54**(11) (2007) 1940–50

8. Marai, G.E.: Data-Driven Predictive Modeling of Diarthrodial Joints. PhD thesis, Brown University (2007)
9. Anderst, W.J., Baillargeon, E., Donaldson, W.F., Lee, J.Y., Kang, J.D.: Validation of a noninvasive technique to precisely measure in vivo three-dimensional cervical spine movement. Spine Phila Pa 1976 **36**(6) (2011) E393–400
10. Haque, M., Anderst, W., Tashman, S., Marai, G.E.: Hierarchical model-based tracking of cervical vertebrae from dynamic biplane radiographs. Medical Engineering & Physics **35**(7) (2013) 994–1004
11. Haque, A., Anderst, W., Tashman, S., Marai, G.: Validation of a non-invasive automated hierarchical method to precisely measure lumbar spine movement. 2012 Annual Meeting of the Orthopaedic Research Society (2012)
12. Mauch, S.: A fast algorithm for computing the closest point and distance transform. SIAM J Sci Comput submitted (2000) 1–17
13. Lorensen, W.E., Cline, H.E.: Marching cubes: A high resolution 3d surface construction algorithm. Computer **21**(4) (1987) 163–169
14. The Numerical Algorithms Group (NAG), Oxford, U.K.: The nag c library (2013). http://www.nag.co.uk/numeric/fl/manual/pdf/E04/e04ccf.pdf
15. Kurtz, S., Edidin, A.: Spine Technology Handbook. Biomedical engineering. Elsevier Science & Technology Books (2006)
16. Yoganandan, N., Kumaresan, S., Pintar, F.: Biomechanics of the cervical spine part 2. cervical spine soft tissue responses and biomechanical modeling. Clin Biomech (Bristol, Avon) **16**(1) (2001) 1–27
17. Przybylski, G., Patel, P., Carlin, G., Woo, S.: Quantitative anthropometry of the subatlantal cervical longitudinal ligaments. Spine **23**(8) (1998) 893–8